Structural and magnetic phenomena in $Ni_{53}Mn_{25}Al_{22}$ thin film prepared by rf magnetron sputtering

Vijay Kumar Srivastava,[1,a)] Saurabh Kumar Srivastava,[1] Ratnamala Chatterjee,[1,b)] Govind Gupta,[2] S. M. Shivprasad,[2] and A. K. Nigam[3]
[1]*Department of Physics, Indian Institute of Technology Delhi, Hauz Khas, New Delhi 110016, India*
[2]*National Physical Laboratory, Dr. K. S. Krishnan Road, New Delhi 110012, India*
[3]*Tata Institute of Fundamental Research, Mumbai 400005, India*

(Received 18 April 2009; accepted 11 August 2009; published online 16 September 2009)

Magnetic and structural properties of Ni–Mn–Al thin films are investigated. It is demonstrated that the annealed film shows $L2_1$ phase at room temperature. Magnetometry measurements reveal that the annealed film is ferromagnetic and a first order transition in magnetization versus temperature measurement confirms that the martensite to austenite transition occurs around room temperature. Transmission electron microscopy measurements confirm that this structural change occurs just below room temperature. The splitting of Mn $2p_{3/2}$ level in x-ray photoelectron spectroscopy core level spectra of the annealed Ni–Mn–Al film, confirms that the origin of magnetism is definitely correlated with the local magnetic moment at the Mn atoms. © *2009 American Institute of Physics*. [doi:10.1063/1.3222940]

Thin films or sheet of stoichiometric/off-stoichiometric full Heusler alloys (HA) (X_2YZ) are of particular interest and are subject of many recent studies because they can be promising candidates for microelectromechanical systems.[1–3] HA films are interesting because of their applications in magnetic tunnel junctions and their unusual optical, magnetic, and magnetotransport properties.[4] Deposition conditions and postdeposition heat treatments are known to affect the magnetic and transport properties of NiMnGa or NiMnAl films. Although reports on thin films of Ni–Mn–Ga (Refs. 2 and 5–9) are numerous, only a few works on Ni–Mn–Al (Refs. 4 and 10) alloy thin films are reported. It has been reported that ferromagnetic and antiferromagnetic states can coexist in stoichiometric Ni_2MnAl alloy and ferromagnetic ordering is typical for off-stoichiometric alloys. It has been observed[11,12] that if the Al based HA sample is to be exploited for its magnetically driven shape memory effect, it is necessary to obtain the alloy in $L2_1$ phase. In this paper, we clearly demonstrate that an annealed Ni–Mn–Al (HA) film with $L2_1$ structure is ferromagnetic in nature and transforms from martensite to austenite phase at around 300 K.

Thin films of Ni–Mn–Al were deposited at ambient temperature under partial pressure of argon (Ar) gas by rf magnetron sputtering. The rf power was adjusted between 300 and 350 W; the base pressure of the sputtering system was 5×10^{-6} mbar and the partial pressure of Ar was optimized for best results. The 7.5 cm diameter target material was prepared by powder compacting high purity (at least 3*N*) Ni, Mn, and Al powders. The atomic ratio of Ni, Mn, and Al powders was optimized so as to get a composition closer to off-stoichiometric $Ni_{53}Mn_{25}Al_{22}$ in the final film. The films were simultaneously deposited on silicon (100), glass, and freshly cleaved potassium chloride (KCl) single crystal substrates. The deposition time was optimized to obtain the films of thickness 100 Å. Subsequently the films were vacuum annealed for 2 h at 423, 523, and 723 K.

Growth process of NiMnAl films have been studied in detail using glancing angle x-ray diffraction (GAXRD), transmission electron microscopy (TEM), energy dispersive x-ray analysis (EDX), and x-ray photoelectron spectroscopy (XPS). The XPS measurements have been performed under high vacuum at a base pressure of 2.6×10^{-10} mbar, using a commercial electron analyzer in a Perkin Elmer machine with Al Kα (1486.6eV) x-ray source. Film composition was estimated from EDX and XPS. XPS was also used to identify the core states of the elements. The magnetic properties of the films were measured using a vibrating sample magnetometer (VSM) make EGG-PAR, Model 155 and superconducting quantum interference device magnetometer (Quantum Design 5T MPMS). TEM measurements were done on Philips CM12.

Figure 1 shows the GAXRD patterns (taken at 300 K) of the films deposited on silicon substrates. Although the as-prepared films do not show $L2_1$ phase, this phase could be stabilized in films annealed at higher temperatures (at 423, 523, and 723 K). Presence of (311), (331), and (422) peaks

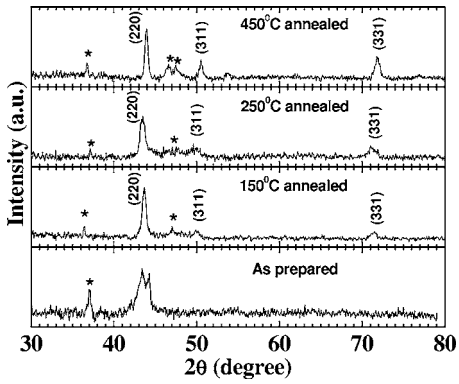

FIG. 1. Glancing angle XRD pattern of the off-stochiometric $Ni_{53}Mn_{25}Al_{22}$ as-prepared and annealed (at 423, 523, and 723 K) thin films on silicon substrates.

[a)]Present address: Department of Aerospace Engineering and Mechanics, University of Minnesota, Minnesota 55455, USA.
[b)]Author to whom correspondence should be addressed. Electronic addresses: rmala@physics.iitd.ac.in and ratnamalac@gmail.com.

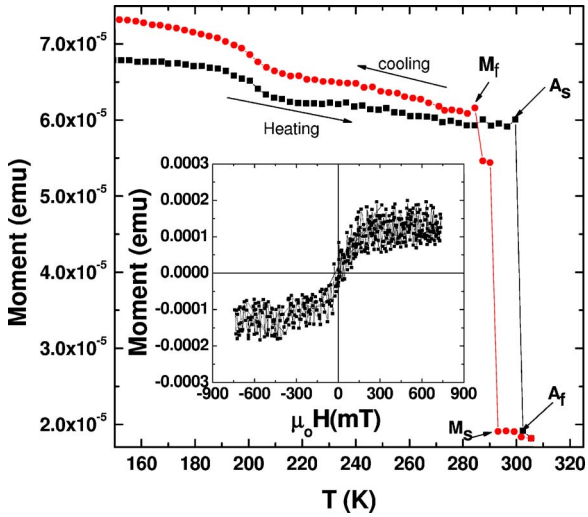

FIG. 2. (Color online) Thermomagnetic cooling and heating curve for the 723 K annealed film in an external field of 100 Oe. The inset shows the magnetic hysteresis loop with in-plane applied magnetic field measured at $T=300$ K.

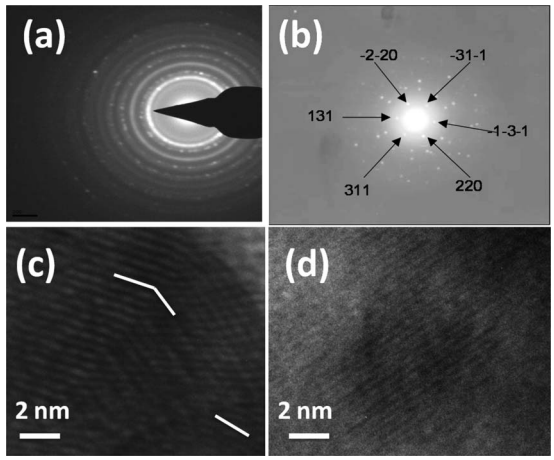

FIG. 3. (a) SAED pattern of 723 K annealed film at 280 K. (b) SAED pattern of the same film at 320K. Sharp diffraction spots depict threefold symmetry. (c) High resolution TEM (HRTEM) micrograph at 280 K on the film. White lines are used to indicate the twin boundaries observed at 280 K. (d) HRTEM image observed at 320 K.

(not indexed in the figure), as shown in Ref. 11, at higher angles are the signatures of $L2_1$ phase; clear evolution of the peaks (311) and (331) on annealing can be observed in this figure. The extra peaks (indicated in Fig. 1 by asterisks) are attributed to the Si substrate.[13] Dominance of the austenitic $L2_1$ (220) peak at $2\theta=43.50°$ in the annealed polycrystalline films suggests a strongly (110)-textured film. The full width at half maximum of the (220) peak can be seen to decrease with higher annealing temperatures. If the peak broadening is solely attributed to grain size, then it is observed that crystallite size increases and crystallinity improves with the increase in annealing temperature. The lattice parameter is calculated as $a=5.997$ Å, using (220) peak; this is in good agreement with the reported values for the bulk samples.

Figure 2 shows the results of the magnetization versus temperature (M-T) measurements performed on a film annealed at 723 K, in the temperature range (5–320 K) at 100 Oe. The data show measurements taken during both heating and cooling cycles. While heating, the thermomagnetic curve drastically decreases at 300 K. The point where the magnetic moment starts decreasing (300 K) is known as austenite start temperature (A_s); this gets completed at 303 K known as austenite finish temperature (A_f). While cooling, once again at 292 K the magnetic moment starts to increase, and this temperature is known as the martensite start temperature (M_s), moment values increase up to 284 K, known as martensite finish temperature (M_f). The important features of the curve are (i) a clear sharp first order phase transition and (ii) a martensitic phase transformation temperature (M_s) estimated to be just below 300 K. The observed decrease in magnetic moment at martensite to austenite transformation is similar to reported results on $Ni_{2+x}Mn_{1-x}Ga$.[14] The M-H measurement for the film was also carried out at room temperature and is shown in inset of Fig. 2. The dc magnetic field was applied perpendicular to the film planes. The ferromagnetic fraction coming from the film is extracted from the raw data by subtracting the diamagnetic slope.

The TEM studies at different temperature were performed on the 723 K films prepared on freshly cleaved KCl. Figure 3(b) shows the selected area electron diffraction (SAED) pattern at 320 K, sharp diffraction spots can be clearly seen. The SAED spot pattern shown here depicts threefold symmetry. Figure 3(b) shows the [110] zone axis of the cubic system. From the measured d spacing the lattice parameter of $a=5.997$ Å was calculated and found to be in close agreement with the lattice constant obtained from the XRD pattern. Both these data further confirm the formation of $L2_1$ phase in the annealed films. A high resolution TEM measurement and SAED pattern taken at 280 K [Figs. 3(a) and 3(c)] indeed reveal clear twin boundaries and a possible lower order (martensitic) structure. Clearly, the 723 K annealed film transforms from martensite to austenite phase just around 300 K. To comprehend the magnetic properties and determination of composition of Ni–Mn–Al thin film, we investigated the Ni, Mn, and Al core level spectra by XPS. The estimated Ni, Mn, and Al atomic percentages are 48%, 27%, and 25%, respectively. This is found to be comparable with our EDX measurement. Here, we discuss the Mn $2p$ core level spectra of the as-deposited and annealed Ni–Mn–Al films as shown in Fig. 4. A broad peak corresponding to the Mn $2p_{3/2}$ core level XPS transition accompanied by a satellite peak toward higher binding energy side is the main characteristic feature in these spectra. The binding energy of the principal Mn $2p_{3/2}$ peak for all the samples falls within 641.6–641.8 eV.

The appearance of a satellite peak is thus a signature of the presence of Mn ions on the surface of thin films. On closer look, an energy splitting of the Mn $2p_{3/2}$ level is visible in the annealed film (marked by arrow in the figure), whereas no such splitting is observed in the as-prepared film. Due to noise in the experimental data, separation between the Mn $2p_{1/2}$ sublevels is not so evident. Magnetic splitting of the Mn $2p_{3/2}$ peak has been observed[15,16] in Co_2MnSn and Pd_2MnSn. This kind of splitting is considered to be the consequence of magnetic ordering in the alloy. Plogmann *et al.*[16] have also shown that the splitting in Mn core level spectra as one goes from Co_2MnAl to Co_2MnSb indicates an exchange splitting for the latter. From the results of XPS measurements one can infer that the exchange splitting of Mn ions possibly is the origin of magnetic moment in this alloy film and the origin of the magnetism is correlated with the local magnetic

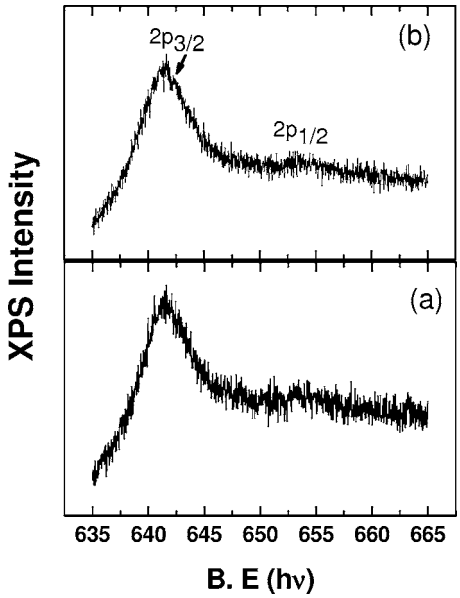

FIG. 4. XPS core level spectra of Mn for (a) as-prepared and (b) annealed film of $Ni_{53}Mn_{25}Al_{22}$ annealed at 723 K.

moment at the Mn atoms. The magnetic behavior of HAs is known to be governed by the interaction of Mn moments and their relative position in the $L2_1$ lattice. First principle calculations by various groups[17–20] have already explained the magnetic behavior of these alloys is a function of the electron concentration e/a; whereas for the martensite structural stability, the Ni $3d$ electrons are decisive.[21] The magnetic behavior in general is governed by the interaction of the Mn moments and depends on the relative position of these atoms ($n.n.$=AF; $n.n.n$=FM) in the $L2_1$ lattice. Thus, the observed Mn $2p_{3/2}$ peak splitting in XPS spectrum of the annealed Ni–Mn–Al thin film verifies that the origin of magnetism in the film is correlated with the local magnetic moment at the Mn atom.

In conclusion, thin film of off-stochiometric Ni–Mn–Al was successfully grown by rf magnetron sputtering. The estimated composition is $Ni_{53}Mn_{25}Al_{22}$. Grain growth with annealing temperature is studied in detail by using XRD, TEM, and atomic force microscopy. It is observed that grain size increases with annealing temperature and the desired $L2_1$ austenite phase (Fm3m space group symmetry) is obtained when the film was annealed at 723 K. VSM measurement clearly shows pure ferromagnetic M-H behavior for annealed films. Increase in saturation magnetization is observed with increase in annealing temperature. M-T measurement clearly shows that at room temperature it transforms from martensite to austenite. The XPS results indicate that the exchange splitting of Mn ions possibly is the origin of magnetic moment in the film.

We would like to acknowledge the referee for his comments. Author would also like to acknowledge the Defense Research Development Organization (DRDO), India for their financial support.

[1] V. A. Chernenko, M. Ohtsuka, M. Kohl, V. V. Khovailo, and T. Takagi, Smart Mater. Struct. **14**, S245 (2005).
[2] M. Kohl, S. Hoffman, Y. Liu, M. Ohtuska, and T. Takagi, J. Phys. IV **112**, 1185 (2003).
[3] K. Bhattacharya and R. D. James, J. Mech. Phys. Solids **47**, 531 (1999).
[4] A. Vovk, M. Yu, L. Malkinski, C. O'Connor, Z. Wang, E. Durant, J. Tang, and V. Golub, J. Appl. Phys. **99**, 08R503 (2006).
[5] M. Kohl, Y. Liu, and M. Ohtsuka, J. Phys. IV **115**, 333 (2003).
[6] M. Ohtsuka, M. Sanada, M. Matsumoto, T. Takagi, and K. Itagaki, Mater. Trans. **44**, 2513 (2003).
[7] M. A. Marioni, R. C. O'Handley, and S. M. Allen, J. Appl. Phys. **91**, 7807 (2002).
[8] J. W. Dong, L. C. Chen, C. J. Palmstrom, R. D. James, and S. McKerman, Appl. Phys. Lett. **75**, 1443 (1999).
[9] J. W. Dong, J. Q. Xie, J. Lu, C. Adalman, C. J. Palmstrom, J. Cui, Q. Pan, T. W. Shield, R. D. James, and S. McKerman, J. Appl. Phys. **95**, 2593 (2004).
[10] X. Y. Dong, J. W. Dong, J. Q. Xie, T. C. Shih, S. McKerenan, and C. Leighton, J. Cryst. Growth **254**, 384 (2003).
[11] V. K. Srivastava and R. Chatterjee, Solid State Commun. **149**, 247 (2009).
[12] A. Fujita, K. Fukamichi, F. Gejima, and R. Kainuma, Appl. Phys. Lett. **77**, 3054 (2000).
[13] J. Giapintzakis, C. Grigorescu, A. Klini, A. Manousaki, V. Zorba, J. Androulakis, Z. Viskadourakis, and C. Fotakis, Appl. Surf. Sci. **197**, 421 (2002).
[14] V. V. Khovailo, V. Novosad, T. Takagi, D. A. Filippov, R. Z. Levitin, and A. N. Vasil'ev, Phys. Rev. B **70**, 174413 (2004).
[15] M. V. Yablonskikh, Y. M. Yarmoshenko, I. V. Solovyev, E. Z. Kurmaev, L. C. Duda, T. Schmitt, M. Magnuson, J. Nordgren, and A. Moewes, J. Electron Spectrosc. Relat. Phenom. **144**, 765 (2005).
[16] S. Plogmann, T. Schlatholter, J. Braun, M. Neumann, Y. M. Yarmoshenko, M. V. Yablonskikh, E. I. Shreder, E. Z. Kurmaev, A. Wrona, and A. Slebarski, Phys. Rev. B **60**, 6428 (1999).
[17] J. Kubler, A. R. Williams, and C. B. Sommers, Phys. Rev. B **28**, 1745 (1983).
[18] S. Ishida, S. Akazawa, Y. Kubo, and J. Ishida, J. Phys. F: Met. Phys. **12**, 1111 (1982).
[19] J. Enkovaara, A. Ayuela, L. Nordstrom, and R. N. Nieminen, Phys. Rev. B **65**, 134422 (2002).
[20] I. Galankis, P. H. Dedrichs, and N. Papanikolaou, Phys. Rev. B **66**, 174429 (2002).
[21] P. Entel, V. D. Buchelnikov, V. V. Khovailo, A. T. Zayak, W. A. Adeagbo, M. E. Gruner, H. C. Herper, and E. F. Wassermann, J. Phys. D: Appl. Phys. **39**, 865 (2006).